2010

# Sulfur K-edge photo-fragmentation of Ethylene Sulfide

Wayne C. Stolte
*University of Nevada, Las Vegas*, wcstolte@lbl.gov

Gunnar Ohrwall
*MAX-lab, Lund University*

# Sulfur K-edge photofragmentation of ethylene sulfide

W. C. Stolte and G. Öhrwall

Citation: J. Chem. Phys. **133**, 014306 (2010); doi: 10.1063/1.3457946
View online: http://dx.doi.org/10.1063/1.3457946
View Table of Contents: http://jcp.aip.org/resource/1/JCPSA6/v133/i1
Published by the American Institute of Physics.

# Sulfur *K*-edge photofragmentation of ethylene sulfide

W. C. Stolte[1,a)] and G. Öhrwall[2]
[1]*Department of Chemistry, University of Nevada, Las Vegas, Nevada 89154-4003, USA and Advanced Light Source, Lawrence Berkeley National Laboratory, Berkeley, California 94720, USA*
[2]*MAX-Lab, Lund University, Box 118, Lund SE-221 00, Sweden*

(Received 17 March 2010; accepted 8 June 2010; published online 7 July 2010)

We have investigated the photofragmentation properties of the three-membered ring heterocyclic molecule ethylene sulfide or thiirane, $C_2H_4S$, by time-of-flight mass spectroscopy. Positive ions have been collected as a function of photon energy around the S *K* ionization threshold. Branching ratios were derived for all detected ions, which are informative of the decay dynamics and photofragmentation patterns of the core-excited species. We present a new assignment of the spectral features around the S *K*-edge. © *2010 American Institute of Physics*.
[doi:10.1063/1.3457946]

## I. INTRODUCTION

Following the creation of a core hole by photoexcitation of a molecule composed of light atoms, valence electrons, which form the chemical bonds, are ejected from the molecule via the dominating Auger process, after which the molecule usually photofragments,[1] dissociating into fragments, ions, and/or neutrals. To understand such photofragmentation processes it is useful to consider the energy regions below and above the ionization threshold separately. Below the threshold, following the excitation of a core electron to a bound unoccupied molecular orbital, a core hole decays via resonant Auger processes.[2,3] Following resonant excitation of shallow core levels, e.g., second row *K*-shells, the valence final states reached are often grouped as due to participator decay and spectator Auger decay. Participator decay is more probable after excitation to virtual molecular orbitals, which are in general less diffuse than Rydberg levels, and lead to relatively long-lived one-hole valence final states. In contrast, spectator Auger decay is more probable after excitation to Rydberg states and leads to a singly charged ion with two valence holes and one electron in an outer diffuse orbital. This type of two-hole one-particle ionic state is more susceptible to dissociate than the one-hole states formed from participator decay. The resulting molecule is often unstable and dissociates into small ionic or neutral fragments. Above the ionization threshold, normal Auger decay dominates, yielding a doubly charged ion that is even more likely to dissociate. For deeper core levels, where the primary decay is dominated by core-core-core type transitions, the role of the excited electron is less obvious. After excitation of a 1*s* electron to an unoccupied orbital in third row elements, the most likely first step in the decay chain is a *KLL* transition, followed by additional *L*-valence-valence electronic decays. The final states will thus typically have a higher charge than after excitation of shallow core levels and the molecule will be more prone to fragment. In the second step, where the two vacancies in the *L*-shell are to be filled, the contraction of the outermost orbitals, due to the increased charge at the core, may well affect the probabilities of participator and spectator decay.

Compared to photoabsorption or absorptionlike measurements, such as total-electron or total-ion yield (including near-edge x-ray-absorption fine structure for gas-phase and adsorbed species), there is a clear advantage in monitoring a channel that is highly selective with respect to different types of resonances.[4–7] Observation of the yield of one particular fragment over a large photon energy range has the advantage to make it possible to emphasize transitions usually hidden (i.e., when ions are not selected in mass and charge) by one or several electronic states with high absorption cross section. The most striking example is the description, resulting from the measurement of negative ions, of doubly excited states above the direct ionization thresholds of the C 1*s* and O 1*s* core orbitals of CO,[4] the two nonequivalent N 1*s* orbitals of $N_2O$ (Ref. 8) and O 1*s* of $CO_2$ (Ref. 7), usually concealed below shape resonances. Another interesting finding derived from partial ion yield spectroscopy is the assessment that below threshold the relative intensity for spectral features related to core-to-Rydberg excitation increases as the fragmentation process is more extended. In other words, for the smaller fragments, the Rydberg states are much more prominent than for the parent molecular ions. This is directly related to spectator decay having a higher probability following excitation to the diffuse Rydberg orbitals, and many or most of the final two hole/one-particle states are dissociative.[9,10]

Three-membered ring compounds have been of great interest to chemists since the discovery of the easy cleavage of cyclopropane single bonds, which was shown to be due to the strain related to the triangular structure. Furthermore, such high degree of strain in these compounds confers upon them properties similar to those of unsaturated compounds. Therefore, the electronic structure and dynamical behavior of heterocyclic three-member ring systems, such as ethylene sulfide, are of interest not only for fundamental studies but also for investigation of many applied chemical and physical phenomena. The photodissociation of ethylene sulfide in the

a)Electronic mail: wcstolte@lbl.gov.

 

ultraviolet regime has been studied by several experiments,[11–14] and there have been two previous x-ray absorption studies involving core excitation around the S *K*-edge.[15,16] In addition to giving a possible spectroscopic assignment, the study by Dezarnaud-Dandine *et al.*[15] investigated the correlation between electron transmission spectroscopy and x-ray absorption spectroscopy. Doomes *et al.*[16] investigated possible correlations between the size of a ring structure and its measured x-ray absorption spectra. We recently studied the fragmentation patterns for two three-membered ring heterocyclic systems: ethylene oxide, $C_2H_4O$, near both the carbon and oxygen *K*-edges, and ethylene sulfide, $C_2H_4S$, near the carbon *K*-edge and sulfur $L_{2,3}$ edges,[17] using total and partial ion yield spectroscopies. Ion mass and charge characterization was done with a 180° hemispherical magnetic sector analyzer with the capability to select fragments with a specific mass and charge.[18] We proposed a spectral assignment for $C_2H_4S$ near the C *K*-edge and the sulfur $L_{2,3}$-edges. In both molecules, we observed high fragmentation efficiency leading to positive and negative ions when exciting these molecules along resonances implying core-to-Rydberg transitions. A state-selective fragmentation pattern leading to the direct production of $S^{2+}$ was analyzed in $C_2H_4S$, which we described in terms of decay of excitations to virtual orbitals to final states above the double ionization threshold.

To the best of our knowledge, no partial-ion-yield experiments near the S *K* ionization threshold have been reported for $C_2H_4S$. Therefore, as an extension of our previous measurements, we have experimentally examined $C_2H_4S$ near the sulfur *K*-edge. The experimental technique used in the present work is different than that of the previous experiment. Namely, we recorded time-of-flight ion spectra as a function of photon energy and derived the branching ratios for the various ionic fragments. In contrast, in the previous experiment we gathered spectra with a magnetic mass analyzer which was set to detect specific ion fragments as a function of photon energy. Using our previous results to interpret the spectral features for this sulfur-containing heterocycle we present a spectral assignment which is different from that proposed by Dezarnaud-Dandine *et al.*,[15] together with a brief analysis for some of the various fragmentation patterns.

## II. EXPERIMENTAL TECHNIQUE

The measurements were performed during two-bunch operations (328 ns period) on bending magnet beamline 9.3.1 at the Advanced Light Source (Lawrence Berkeley National Laboratory, Berkeley, CA, USA). Calibration at the S 1*s*-edge was performed by comparison to Reynaud *et al.*[19] using the S $(1s)^{-1} \rightarrow 6t_u$ transition in $SF_6$ at 2486.0 eV. We estimated the flux of the incident radiation near the S *K*-edge to be approximately $4 \times 10^{10}$ photons/s, with a resolution of 0.4 eV by comparison to our recent measurements near the S $(1s)^{-1} \rightarrow 6a_1 3b_2^*$ transition in $H_2S$.[20]

The branching ratios were measured with a time-of-flight mass spectrometer which was used in the space focusing mode,[21] under conditions similar to our previous experimental setup.[22,23] A sample time-of-flight spectrum is shown in Fig. 1, which was recorded on top of the $a_1$ and $b_1$ resonance located at 2471.88 eV. The total distance traveled by the ions was about 8 cm. Due to the 328 ns bunch structure of the storage ring, we had to carefully choose the voltages on the various elements so that there would be no overlap in the relative time of the various ions. The heavier ions required several 328 ns time periods to arrive at the detector, whereas, hydrogen arrived in approximately 210 ns. In addition, to keep a constant efficiency, the ions were also required to have sufficient energy such that they strike the front surface of the microchannel plate (MCP) with an energy between 4 and 5 keV. As can be seen in Fig. 1, hydrogen appears near the center of the spectrum. We could have time shifted the entire spectrum with a time delay, but this would have caused loss of some information during the 20 ns of dead time which occurred during the time-to-amplitude converter (TAC) reset time (between 8000 and 0 in Fig. 1). The output pulses from the MCP were fed into conventional electronic counting equipment, with constant fraction discriminators being used to suppress any electronic noise. In all cases the discrimination level was kept as low as possible, with the levels being verified by comparing the branching ratios for hydrogen and sulfur on resonance while varying the discriminator setting. Gas pressure was kept in the mid-$10^{-6}$ Torr range. The dwell time at each data point was sufficient to provide counting statistics in the 1%–3% range. The ion signal was used to start the TAC, and a signal from the synchrotron ring provided a reliable stop pulse for the TAC. A multihit TAC was not used in this experiment, therefore, coincidence measurements between the various ions were not feasible.

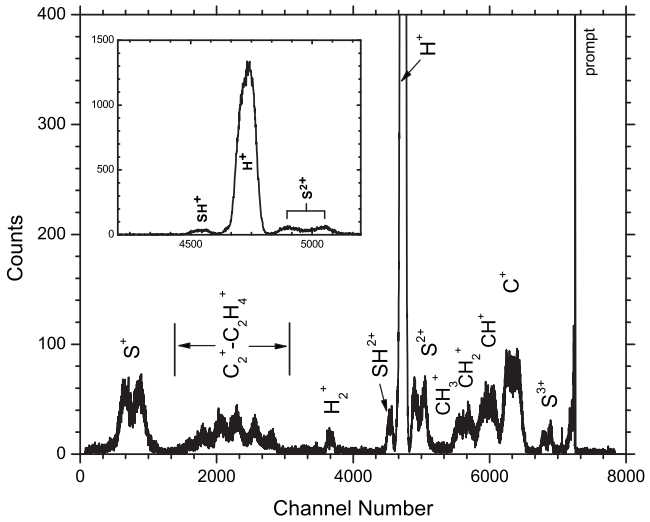


FIG. 1. Time-of-flight spectrum taken on top of the $a_1$ and $b_1$ resonance (2471.88 eV).

The presented total-ion-yield spectrum (see Fig. 2) was measured using a static gas cell, containing 200 mTorr of gas. The cell was closed on one side with a 7.6 $\mu$m thick Kapton® (E.I. du Pont de Nemours and Co., Wilmington, DE) window of 10 mm diameter, which was preceded in the beamline by an aluminized Mylar foil which was used to measure $I_0$. Inside the static gas cell, the ions were measured

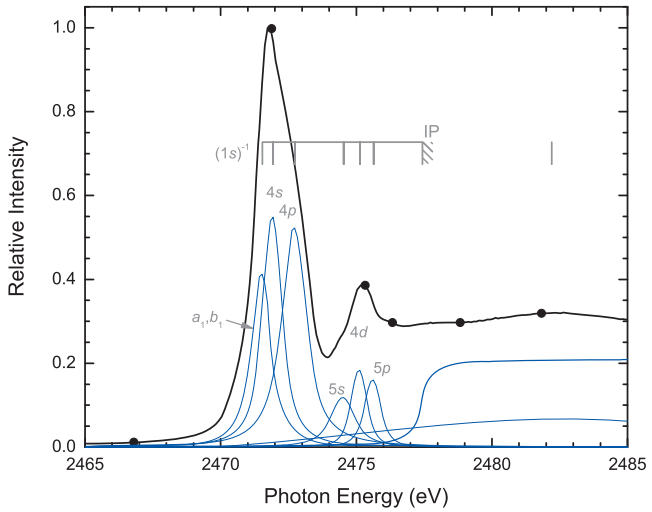


FIG. 2. Total-ion-yield spectrum, normalized to equal one on top of the first strong resonance (2471.88 eV) after removing the pre-edge signal. Dots denote locations for branching ratio values given in Tables II and III. The blue curves represent the peaks resulting from fitting of the TIY spectrum.

with a 20 cm long parallel plate spectrometer. The ions were steered onto and collected on one of the parallel plates, while the opposite plate was kept at +200 direct current voltage (DCV). The ion current was monitored with a Keithley model 6517A electrometer (Keithley Instruments, Inc., Cleveland, OH).

The ethylene sulfide was commercially obtained as a 99% pure liquid from Sigma Aldrich. The sample was purged of contaminants by performing a minimum of three freeze/thaw cycles while pumping out the excess vapors from the frozen sample with a mechanical pump and finally introduced into the chamber after thawing by using its vapor pressure at room temperature.

## III. RESULTS

Previously the valence electronic structure of ethylene sulfide was investigated by He(I) and He(II) photoelectron spectroscopy,[24] and there have been two x-ray absorption studies involving core excitation around the S *K*-edge.[15,16] These two studies do not agree upon a spectroscopic assignment. We therefore assumed that the orbital ordering and composition for $C_2H_4S$ are analogous to the $C_2H_4O$ system, and just as in our previous paper,[17] we compared the present results to the spectral assignment for $C_2H_4O$ near the O *K*-edge.

As can be seen in Fig. 2, the general appearance of the absorption curve is very similar to that of the oxygenated analog (see Refs. 17 and 25). This similarity allows us to use a spectral assignment, shown in Table I, similar to the one we adopted at the sulfur $L_{2,3}$-edges, but which is different from that proposed by Dezarnaud-Dandine *et al.*[15] A detailed assignment of all members of the Rydberg series would be rather speculative and would require detailed theoretical calculations, which do not exist; we therefore suggest only a general attribution to transitions to either virtual molecular orbitals or Rydberg levels. The first spectral feature with maximum at 2471.65 eV accounts for the transitions from

TABLE I. Observed energies, $\delta$, and term values, for excitation of S 1*s* electrons in $C_2H_4S$ to $a_1$ and $b_1$ valence states and the Rydberg orbitals. All values are relative to the $SF_6$ $1s^{-1} \rightarrow 6t_u$ transition at 2486.0 eV (Ref. 19), which has an estimated 0.1 eV systematic error in photon energy reproducibility. " * " denotes ionization energy as given in Ref. 15.

| Suggested assignment | Present measurement (eV) | $\delta$ | Term value (eV) | Reference 15 (eV) |
|---|---|---|---|---|
| $(1s^{-1})a_1,b_1$ | 2471.5 ± 0.2 | ⋯ | ⋯ | ⋯ |
| 4*s* | 2471.9 ± 0.2 | 2.43 | 5.6 | 2472.0 |
| 4*p* | 2472.7 ± 0.2 | 2.31 | 4.8 | 2472.8 |
| 5*s* | 2474.5 ± 0.2 | 2.83 | 2.9 | ⋯ |
| 4*d* | 2475.1 ± 0.2 | 1.57 | 2.3 | 2475.3 |
| 5*p* | 2475.6 ± 0.2 | 2.25 | 1.8 | ⋯ |
| IP* | 2477.4 | ⋯ | ⋯ | 2477.4 |
| ⋯ | 2482.2 ± 0.3 | ⋯ | ⋯ | 2482 |

the S 1*s* level to the lowest-lying virtual molecular orbitals, which were assigned as $a_1$, $b_1$, and 4*s*. The following spectral features correspond to transitions to level with pure Rydberg character (4*p*, 5*s*, 4*d*, and 5*p*, in analogy with $C_2H_4O$). The peak positions were estimated by using 2477.4 eV as the ionization potential[15] subsequently fitting the total-ion-yield spectrum with WinXAS©(Thorsten Ressler, Hamburg, Germany) (Ref. 26) and its near edge x-ray absorption fitting routines, resulting in the $\delta$ and Rydberg term values given in Table I.

We have detected a wealth of fragments in the photon energy region: $S^+$, $S^{2+}$, $S^{3+}$, $C_2H_x^+$, $CH_2^+$, $CH^+$, $C^+$, $H^+$, and $H_2^+$ shown in Fig. 3; $C_2H_4^+$, $C_2H_3^+$, $C_2H_2^+$, $C_2H^+$, $C_2^+$, and their sum $C_2H_x^+$ are shown in Fig. 4. We did observe $SH^{2+}$, but we do not show it here because it was only very weakly seen in the few measurements taken between the $a_1$ and $b_1$ resonance and the ionization threshold. Table II presents an abbreviated list of the branching ratios shown in Fig. 3. There is an estimated 1%–3% statistical error and approximately 5% systematic error for branching ratios 10% and larger. For results smaller than 10%, the combined error is 10%–12%, except for the $H_2^+$ ion which due to its weak

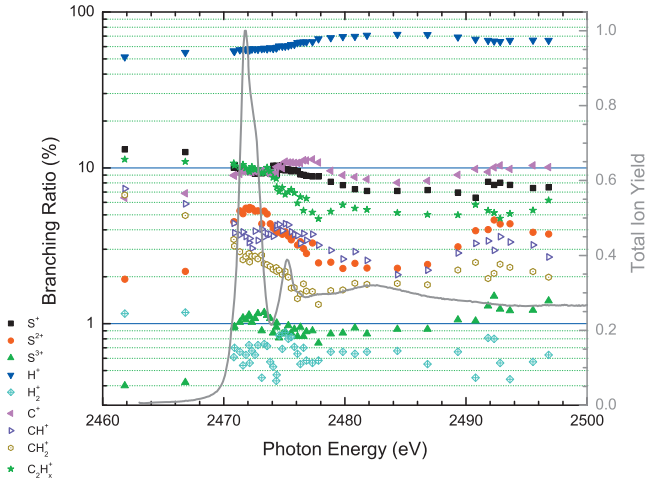


FIG. 3. Branching ratios following photoexcitation of $C_2H_4S$ near the S 1*s* ionization threshold. The TIY, which was normalized to equal one on top of the first strong resonance (2471.88 eV) after removing the pre-edge signal, is added for comparison.

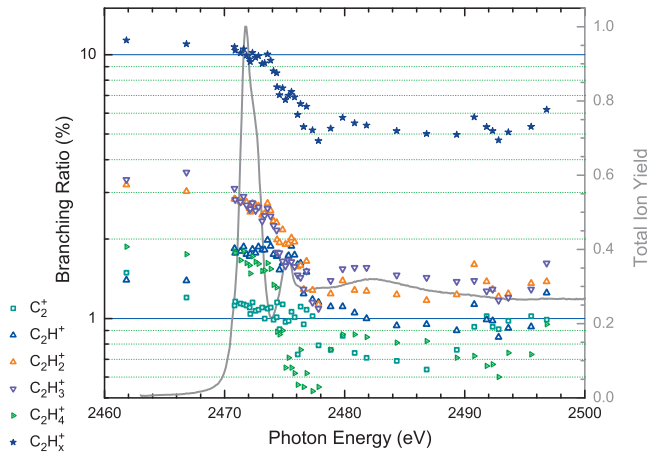


FIG. 4. Estimated branching ratios for the $C_2H_x^+$ series, following photoexcitation of $C_2H_4S$ near the S 1*s* ionization threshold. The TIY, which was normalized to equal one on top of the first strong resonance (2471.88 eV) after removing the pre-edge signal, is added for comparison.

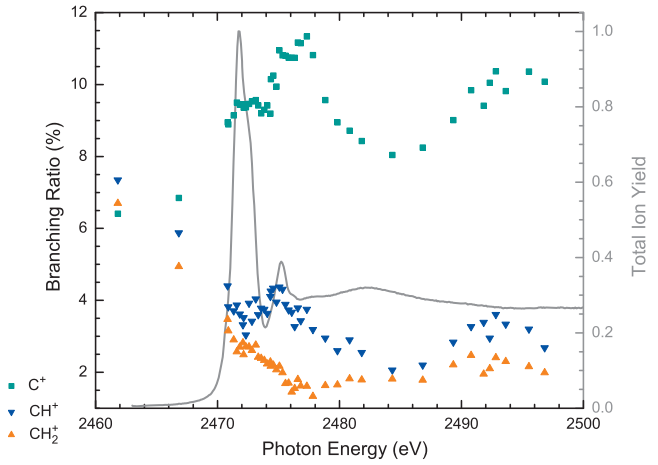


FIG. 5. Comparison of branching ratios for $CH_2^+$, $CH^+$, and $C^+$ following photoexcitation of $C_2H_4S$ near the S 1*s* ionization threshold. The TIY, which was normalized to equal one on top of the first strong resonance (2471.88 eV) after removing the pre-edge signal, is added for comparison.

signal has 20% error. Presented separately in Table III are the estimated branching ratios for the ion fragment series $C_2^+$, $C_2H^+$, $C_2H_2^+$, $C_2H_3^+$, $C_2H_4^+$, and their sum $C_2H_x^+$, at the same energies as the ones presented in Table II. Due to their weak signal and their broad peak shapes, a combined estimated statistical and systematic error of 15% should be applied for all of these branching ratios, except for the sum $C_2H_x^+$, which due to the increased combined counting rate has an estimated 10% total error.

Some interesting experimental findings are evident from the comparison between the total ion yield (TIY) and the branching ratios of the various fragment ions. If we compare the total yield and the branching ratios for a sequence of ion fragments corresponding to a subsequent fragmentation process, namely, $CH_2^+$, $CH^+$, and $C^+$, which are shown in Fig. 5, we notice that the relative intensity of the spectral features related to transitions to the Rydberg series region increases as the fragment ion becomes lighter. This is in contrast with the large broad structure related to transitions to empty molecular orbitals, over which the branching ratios stay relatively constant. This effect has been reported by us for several other systems, methyl chloride,[10] acetylene, and ethylene,[9] and most recently for both ethylene oxide and ethylene sulfide.[17] In these cases, the explanation is that the final states are reached after resonant Auger decay from core-excited states where the excited electron is promoted to a virtual molecular orbital or to a Rydberg orbital. For excitation to a virtual molecular orbital the most likely decay processes are participator decay, which then leads to relatively long-lived one-hole valence final states. For primary excitation involving Rydberg states, the system with one electron in an orbital far from the ionic core preferentially relaxes by spectator Auger decay, and the singly charged ion with two valence holes and one electron in an outer diffuse orbital remains in an excited state more susceptible to dissociation. Surprisingly enough, even though in the case of a S 1*s* vacancy, the dominant decay path is *KLL* Auger, followed by subsequent cascade processes, the presence of an electron in a virtual molecular orbital or a Rydberg orbital influences the fragmentation in a similar way. Again as we observed for acetylene and ethylene,[9] the broad resonance located above the ionization threshold appears to shift toward higher energy as the fragment ion gets lighter. This is most likely due to more vibrational and/or electronic energy being stored in the intermediate state as the exciting photon energy is increased. Interestingly enough, these effects are not clearly observed for the other detected sequence of ion fragments, namely, the $C_2H^+$ series, which are compared in Fig. 4. In this case, even

TABLE II. Observed branching ratios for fragment ions from $C_2H_4S$ at some selected photon energies near the S 1*s* ionization threshold. Branching ratios of 10% or larger have estimated counting statistics of 1% to 3% and 5% systematic error. Branching ratios smaller than 10% have 10%–12% combined error except $H_2^+$ which has a 20% combined error.

| Photon energy (eV) | Branching ratio (%) | | | | | | | | | |
|---|---|---|---|---|---|---|---|---|---|---|
| | $S^+$ | $S^{2+}$ | $S^{3+}$ | $H^+$ | $H_2^+$ | $C^+$ | $CH^+$ | $CH_2^+$ | $C_2H_x^+$ | $SH^{2+}$ |
| 2466.8 | 12.6 | 2.2 | 0.4 | 55.0 | 1.2 | 6.9 | 5.9 | 4.9 | 11.0 | 0 |
| 2471.88 | 9.6 | 5.4 | 1.1 | 57.5 | 0.6 | 9.3 | 3.5 | 2.7 | 10.0 | 0.3 |
| 2475.33 | 9.8 | 3.7 | 1.0 | 60.7 | 0.8 | 10.8 | 4.3 | 2.0 | 7.0 | 0 |
| 2476.33 | 9.1 | 3.4 | 1.0 | 64.0 | 0.6 | 10.7 | 3.3 | 1.6 | 6.5 | 0 |
| 2478.83 | 8.2 | 2.5 | 0.9 | 68.4 | 0.7 | 9.6 | 3.0 | 1.6 | 5.3 | 0 |
| 2481.83 | 7.1 | 2.3 | 0.9 | 70.9 | 0.7 | 8.4 | 2.6 | 1.8 | 5.4 | 0 |
| 2493 | 7.4 | 3.8 | 1.2 | 66.6 | 0.6 | 9.8 | 3.1 | 2.1 | 5.4 | 0 |

TABLE III. Estimated branching ratios for $C_2^+$, $C_2H^+$, $C_2H_2^+$, $C_2H_3^+$, and $C_2H_4^+$ fragment ions, and their sum $C_2H_x^+$ from photoexcitation of $C_2H_4S$ near the S 1*s* ionization threshold. Estimated combined statistical error and systematic error of 15% for all except $C_2H_x^+$ (estimated 10% combined error).

| Photon energy (eV) | Branching ratio (%) | | | | | |
|---|---|---|---|---|---|---|
| | $C_2H_x^+$ | $C_2^+$ | $C_2H^+$ | $C_2H_2^+$ | $C_2H_3^+$ | $C_2H_4^+$ |
| 2466.8 | 11.0 | 1.2 | 1.4 | 3.0 | 3.6 | 1.8 |
| 2471.88 | 10.0 | 1.1 | 1.8 | 2.7 | 2.7 | 1.6 |
| 2475.33 | 7.0 | 1.0 | 1.7 | 1.9 | 1.7 | 0.7 |
| 2476.33 | 6.5 | 1.1 | 1.6 | 1.6 | 1.4 | 0.8 |
| 2478.83 | 5.3 | 0.8 | 1.1 | 1.2 | 1.4 | 0.8 |
| 2481.83 | 5.4 | 0.7 | 1.0 | 1.3 | 1.6 | 0.9 |
| 2493 | 5.4 | 1.0 | 1.0 | 1.3 | 1.3 | 0.8 |

taking into account the larger error, the branching ratio curves for all of the fragment ions have a similar shape, but with an enhancement of the higher level Rydberg transitions in the fragments with fewer hydrogen atoms.

In Fig. 6 we compare three positively charged fragments whose branching ratios are particularly interesting, namely, $S^+$, $S^{2+}$, and $S^{3+}$. We can immediately observe that the $S^+$ and $S^{2+}$ ratios are very different, the singly ionized state slowly decaying with increasing photon energy, whereas both the doubly and triply charged ions rapidly peak on the $a_1$ and $b_1$ resonance, and decay over the Rydberg region, more closely mimicking the TIY curve. This implies that the singly charged ions derive from a different fragmentation processes than the higher charged states. An explanation for this is that the $S^+$ ion is primarily a result of valence photoionization rather than being due to relaxation of the core-hole, and $S^{2+}$, and $S^{3+}$ increase dramatically on resonance because of multistep processes such as Auger cascade following the filling of the S 1*s* core-hole with electrons from the S 2*p* shell. Further indication for these fragmentation processes is the double peaks observed in the time-of-flight spectra shown in Fig. 1, most easily seen on resonance for the $S^+$ and $S^{2+}$ ions. A time-of-flight spectrum recorded 30 eV above resonance (not shown here) shows single peaks for each of the sulfur ions, with an identical baseline width as the split peak features observed on resonance (Fig. 1). This behavior is a reflection of our time-of-flight analyzer being aligned parallel to the polarization vector of the synchrotron beam.[23] A preferential absorption of the incident photons occurs when the resonantly excited orbital with a well defined symmetry, either $a_1$ or $b_1$, is aligned parallel to the exciting photon beam polarization vector. The ions are created following explosion of the highly ionized molecule, ejected with a specific kinetic energy. Due to the molecules alignment with respect to the beamline polarization, the ions are ejected toward or away from the detector. Those ejected toward the detector arrive in a shorter time, those ejected away arrive later, resulting in double peaks. Because the hydrogen atoms lie outside of the molecules $C_{2v}$ symmetry axis, the lightest fragment ion $H^+$ does not exhibit this behavior. Another less likely direct mechanism to create $S^{2+}$ and $S^{3+}$ was observed between these very same fragment ions at the S $L_{2,3}$-edge.[17] Primarily created by participator decay, the $S^{2+}$ ion fragment could stem from a valence doubly charged molecular state, with some of the states being located above the double ionization threshold. This state can then fragment, directly producing a doubly charged fragment. Unlike spectator Auger decay, participator decay is more probable after excitation to virtual molecular orbitals, which in general are less diffuse than Rydberg levels, thus leading to relatively long-lived one-hole valence final states. One would need to perform energy resolved photoelectron-photoion coincidence measurements to prove if any multiply charged sulfur was created by this direct mechanism.

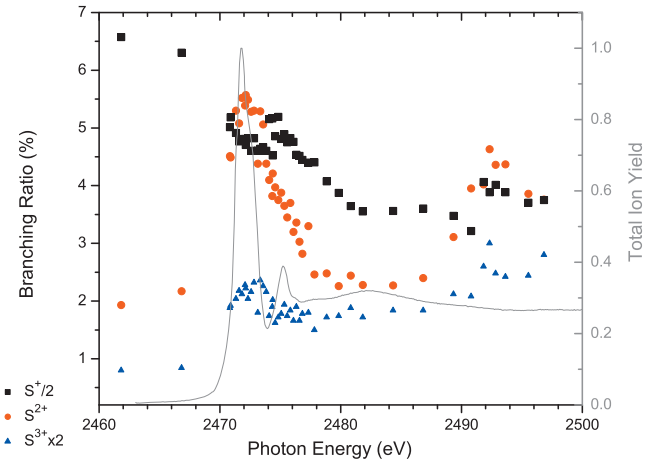


FIG. 6. Comparison of branching ratios for $S^{2+}$ and $S^{3+}$ following photoexcitation of $C_2H_4S$ near the S 1*s* ionization threshold. The TIY, which was normalized to equal one on top of the first strong resonance (2471.88 eV) after removing the pre-edge signal, is added for comparison.

## IV. CONCLUSION

We have performed branching ratio experiments near the S 1*s* threshold to further investigate the photofragmentation patterns of the three-membered ring heterocyclic molecule ethylene sulfide. Based on our previous results, we have proposed an assignment of the observed spectral features. Similarly to what we observed at the S 2*p* and C 1*s* thresholds, high fragmentation efficiency is seen when exciting this molecule along resonances involving core-to-Rydberg transitions. A state-selective fragmentation pattern which leads to the direct production of $S^{2+}$ was analyzed, which is described

in terms of decay of excitations to virtual molecular orbitals to final states above the double-ionization threshold.

## ACKNOWLEGEMENTS

The authors thank the staff of the ALS for their excellent support. We would also like to thank M. N. Piancastelli for her help with the preparation of this manuscript. Support from the National Science Foundation under NSF Grant No. PHY-05-55699 is gratefully acknowledged. The Advanced Light Source is supported by DOE (Grant No. DE-AC03-76SF00098).

[1] I. Nenner and P. Morin, in *VUV and Soft X-Ray Photoionization*, edited by U. Becker and D. A. Shirley (Plenum, New York, 1996), p. 291.
[2] J. Kikuma and B. P. Tonner, J. Electron Spectrosc. Relat. Phenom. **82**, 41 (1996).
[3] S.-Y. Chen, C.-I. Ma, D. M. Hanson, K. Lee, and D. Y. Kim, J. Electron Spectrosc. Relat. Phenom. **93**, 61 (1998).
[4] W. C. Stolte, D. L. Hansen, M. N. Piancastelli, I. Dominguez Lopez, A. Rizvi, O. Hemmers, H. Wang, A. S. Schlachter, M. S. Lubell, and D. W. Lindle, Phys. Rev. Lett. **86**, 4504 (2001).
[5] W. C. Stolte, G. Öhrwall, M. M. Sant'Anna, I. Dominguez Lopez, L. T. N. Dang, M. N. Piancastelli, and D. W. Lindle, J. Phys. B **35**, L253 (2002).
[6] D. L. Hansen, W. C. Stolte, O. Hemmers, R. Guillemin, and D. W. Lindle, J. Phys. B **35**, L381 (2002) (and references therein).
[7] G. Öhrwall, M. M. Sant'Anna, W. C. Stolte, I. Dominguez Lopez, L. T. N. Dang, A. S. Schlachter, and D. W. Lindle, J. Phys. B **35**, 4543 (2002).
[8] S.-W. Yu, W. C. Stolte, G. Öhrwall, R. Guillemin, M. N. Piancastelli, and D. W. Lindle, J. Phys. B **36**, 1255 (2003).
[9] M. N. Piancastelli, W. C. Stolte, G. Öhrwall, S.-W. Yu, D. Bull, K. Lantz, A. S. Schlachter, and D. W. Lindle, J. Chem. Phys. **117**, 8264 (2002).
[10] D. Céolin, M. N. Picancastelli, R. Guillemin, W. C. Stolte, S.-W. Yu, O. Hemmers, and D. W. Lindle, J. Chem. Phys. **126**, 084309 (2007).
[11] H. L. Kim, S. Satyapal, P. Brewer, and R. Bersohn, J. Chem. Phys. **91**, 1047 (1989).
[12] F. Qi, O. Sorkhabi, and A. G. Suits, J. Chem. Phys. **112**, 10707 (2000).
[13] F. Qi, O. Sorkhabi, A. G. Suits, S.-H. Chien, and W.-K. Li, J. Am. Chem. Soc. **123**, 148 (2001).
[14] S.-Y. Chiang and Y.-S. Fang, J. Electron Spectrosc. Relat. Phenom. **144–147**, 223 (2005).
[15] C. Dezarnaud-Dandine, F. Bournel, C. Mangeney, M. Tronc, A. Modelli, and D. Jones, Chem. Phys. **265**, 105 (2001).
[16] E. E. Doomes, R. L. McCarley, and E. D. Poliakoff, J. Chem. Phys. **119**, 4399 (2003).
[17] W. C. Stolte, I. Dumitriu, S.-W. Yu, G. Öhrwall, M. N. Picancastelli, and D. W. Lindle, J. Chem. Phys. **131**, 174306 (2009).
[18] W. C. Stolte, R. Guillemin, S.-W. Yu, and D. W. Lindle, J. Phys. B **41**, 145102 (2008).
[19] C. Reynaud, S. Bodeur, J. L. Maréchal, D. Bazin, P. Millié, I. Nenner, U. Rockland, and H. Baumgätel, Chem. Phys. **166**, 411 (1992).
[20] L. Journel *et al.* (unpublished).
[21] W. C. Wiley and I. H. McLaren, Rev. Sci. Instrum. **26**, 1150 (1955).
[22] J. A. R. Samson, W. C. Stolte, Z.-X. He, J. N. Cutler, Y. Lu, and R. J. Bartlett, Phys. Rev. A **57**, 1906 (1998).
[23] D. L. Hansen, M. E. Arrasate, J. Cotter, G. R. Fisher, O. Hemmers, K. T. Leung, J. C. Levin, R. Martin, P. Neill, R. C. C. Perera, I. A. Sellin, M. Simon, Y. Uehara, B. Vanderford, S. B. Whitfield, and D. W. Lindle, Phys. Rev. A **58**, 3757 (1998).
[24] A. Schweig and W. Thiel, Chem. Phys. Lett. **21**, 541 (1973).
[25] K. H. Sze and C. E. Brion, J. Electron Spectrosc. Relat. Phenom. **57**, 117 (1991).
[26] T. Ressler, see: http://www.winxas.de/, 2009.